Mineral equilibria and thermodynamic uncertainties in the geothermometrical characterisation of carbonate geothermal systems of low temperature. The case of the Alhama-Jaraba system (Spain)

Mónica Blasco[a]*, Luis F. Auqué[a], María J. Gimeno[a], Particia Acero[a], Javier Gómez[a], Maria P. Asta[b]

[a] Geochemical Modelling Group. Petrology and Geochemistry Area, Earth Science Department, University of Zaragoza, Spain C/ Pedro Cerbuna 12, 50009 Zaragoza, Spain.

[b] Environmental Microbiology Laboratory (EML), École Polytechnique Fédérale de Lausanne (EPFL). EPFL-ENAC-IIE-EML. Station 6, 1015, Lausanne, Switzerland.

* Corresponding author: Geochemical Modelling Group. Petrology and Geochemistry Area, Earth Sciences Department, University of Zaragoza, Spain. E-mail: monicabc@unizar.es; Tel.: +34 976761071; Fax: +34 976761106.

Abstract

Geothermometrical characterisation of low-temperature, carbonate-evaporitic geothermal systems is usually hampered by the lack of appropriate mineral equilibria to successfully use most of the classical geothermometers and/or by the thermodynamic uncertainties affecting some of the most probable mineral equilibria in low temperature conditions. This situation is further hindered if the thermal waters are additionally affected by secondary processes (e.g., CO_2 loss) during their ascent to surface.

All these problems cluster together in the low-temperature Alhama-Jaraba thermal system, hosted in carbonate rocks, with spring temperatures about 30 ºC and waters of Ca-Mg-HCO_3/SO_4 type. This system, one of the largest naturally flowing (600 L/s) low temperature thermal systems in Europe, is used in this paper as a suitable frame to assess the problems in the application of chemical geothermometrical techniques (classical geothermometers and geothermometrical modelling) and to provide a methodology that could be used in this type of geothermal system or in potential CO_2 storage sites in similar aquifers.

The results obtained have shown that the effects of the secondary processes can be avoided by selecting the samples unaffected by such processes and, therefore, representative of the conditions at depth, or by applying existing methodologies to reconstruct the original composition, as is usually done for medium to high temperature systems.

The effective mineral equilibria at depth depend on the temperature, the residence time and the specific lithological/mineralogical characteristics of the system studied. In the present case, the mineral equilibria on which classical cation geothermometers are based have not been attained. The low proportion of evaporitic minerals in the hosting aquifer prevents the system from reaching anhydrite equilibrium, otherwise common in carbonate-evaporitic systems and necessary for the specific SO_4-F geothermometer or the specially reliable quartz (or chalcedony) – anhydrite equilibrium in the geothermometrical modelling of these geothermal systems.

Under these circumstances, the temperature estimation must rely on quartz (or chalcedony), clay minerals and, especially, calcite and dolomite phases. However, clay minerals and dolomite present important thermodynamic uncertainties related to possible variations in composition or crystallinity degree for clays and order/disorder degree for dolomite.. To deal with these problems, a sensitivity analysis to the thermodynamic data for clay minerals has been carried out, comparing the results obtained when considering different solubility data. The uncertainties associated with dolomite have been addressed by reviewing the solubility data available for dolomites with different order degrees

and performing specific calculations for the order degree of the dolomite in the aquifer. This approach can be used to find the most adequate dolomite thermodynamic data for the system under consideration, including medium-high temperature geothermal systems.

Finally, the temperature estimation of the Alhama-Jaraba waters in the deep reservoir has been obtained from simultaneous equilibria of quartz, calcite, partially disordered dolomite and some aluminosilicate phases. The obtained value of 51 ± 14 ºC is within the uncertainty range normally affecting this type of estimations and is coherent with independent estimations from geophysical data.

Keywords: Low temperature geothermal system; Geothermometry; Geothermometrical modelling; Calcite-dolomite equilibrium; Carbonate aquifer

1. INTRODUCTION

A wide variety of geothermometrical techniques are available to evaluate the reservoir temperature of thermal waters: various chemical and isotopic solute geothermometers and the geothermometrical modelling (or multicomponent solute geothermometry; e.g. Spycher et al., 2014). However, not all of them are always applicable to all thermal systems and they should be carefully selected according to the different equilibria expected at depth.

In the case of low temperature thermal systems hosted in carbonate rocks, a series of problems arise when applying the geothermometrical techniques due to three main reasons: 1) the low temperatures usually make difficult the attainment of the mineral and/or isotopic equilibria; 2) the mineral set present in the reservoir is usually more limited (mainly calcite and dolomite) than in other type of geothermal systems; and 3) the thermodynamic properties of dolomite and clays are uncertain.

An additional complication in the evaluation of the reservoir temperature in any thermal system is the presence of secondary processes during the rising of the thermal waters to the surface (e.g. mixing

with colder and shallower waters, re-equilibrium processes through mineral-water reactions and/or CO_2 outgassing).

The work presented in this paper is focused on the use and evaluation of several geothermometrical tools in order to calculate the reservoir temperature of the geothermal system of Alhama de Aragón – Jaraba (from now on, Alhama–Jaraba). The characteristics of this thermal system provide the opportunity to deal with almost all the aforementioned complexities (Tena et al., 1995; Auqué et al., 2009; Blasco et al. 2016): 1) the reservoir is hosted mainly in carbonate rocks (limestones and dolostones), 2) the temperature is, a priori, low and 3) there are different secondary processes (mixing, CO_2 outgassing) affecting the chemistry of some of the waters. There are other reasons why the study of this system presents a special interest. One is the importance of the system as a natural resource with very high flow rates (550 L/s in Alhama and 600 L/s in Jaraba; IGME, 1980; De Toledo and Arqued, 1990; Sánchez et al., 2004) comparable to those found in the area considered the Europe's largest naturally flowing thermal system in Budapest (discharge of ca. 580 L/s; Goldscheider et al., 2010 and references therein). The other reason is related to its special geological and hydrogeochemical features which have given it the consideration of a natural analogue for the CO_2 geological storage (Auqué et al. 2009).

In summary, this study gives a suitable natural frame to test different geothermometrical techniques and the associated uncertainties in low temperature systems hosted in carbonate rocks. From this, a general methodology can be established to be applied in this type of geothermal systems and even in the characterisation of some potential CO_2 storage sites in similar aquifers.

2. GEOLOGICAL, HYDROGEOLOGICAL AND HYDROGEOCHEMICAL SETTING

The Alhama de Aragón and Jaraba springs (NE Spain, Figure 1) belong to one of the main thermal systems in Spain. There are several thermal resorts and water bottling plants in the area at present. The

Jaraba thermal complex, close to the Mesa River, consists of 14 catalogued springs flowing at an elevation of 737 m.a.s.l. and the Alhama thermal complex, located close to the Jalón River bank, is formed by a dozen of catalogued springs flowing at an elevation of 660 m. Apart from these well-known spring complexes, there are another two minor hot springs in the nearby area, Embid and Deza springs (Tena et al., 1995; Sanz and Yélamos, 1998; Sánchez et al., 2004; Auqué et al., 2009; Figure 1), which have not been included in this study.

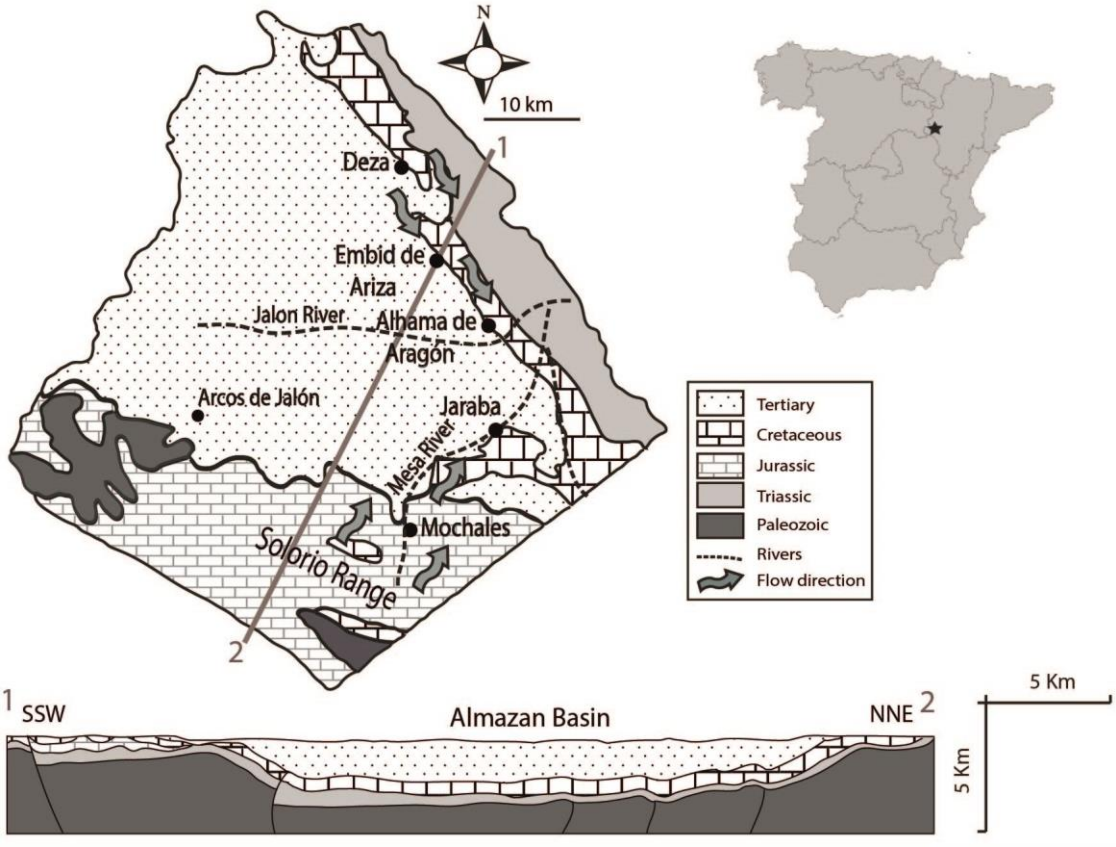

Figure 1. Location of the Alhama de Aragón and Jaraba geothermal systems in the geological map (modified form Sánchez et al., 2004) and a cross section showing the main structural and lithological characteristics of the area studied (modified from the ALGECO2 project; IGME, 2010).

Geologically, the Alhama-Jaraba thermal system is located on the border of the Western Iberian Range and the tertiary Almazán Basin (Figure 1). There are two main aquifers in this area: 1) the Solorio aquifer, hosted in the Jurassic carbonate formations; and 2) the Alhama aquifer, hosted in the Upper

Cretaceous carbonate rocks. The hydrological model of the region is not completely clear, but the most accepted hypothesis states that there are two possible recharge areas located 1) in the Solorio Range with a flow direction SW-NE towards Jaraba and Alhama (Figure 1) and 2) in the vicinity of Deza, with a NW-SE flow direction towards Embid and Alhama (Figure 1; IGME, 1980; 1987; De Toledo and Arqued, 1990; Sanz and Yelamos, 1998; Sánchez et al., 2000; Sanchez et al., 2004). The fact that the rocks in the Solorio recharge area are mainly Jurassic and that all the thermal springs are associated with the Upper Cretaceous formations (Sánchez et al., 2000) suggests that both aquifers could be connected and that their emergence would be related to the presence of vertical or near vertical layers that allow a rapid ascent of the water from depth (Sánchez et al., 2004).

The mineralogy of the Jurassic and Cretaceous carbonate rocks is quite similar. The rocks are mainly dolostones and limestones with dispersed anhydrite/gypsum intercalations (Meléndez et al., 1985; Alonso et al., 1993; Aurell, et al., 2002). The Cretaceous formations are locally affected by a silicification processes with development of authigenic quartz crystals (Meléndez et al., 1985) and there are also intercalations of terrigenous rocks, mainly at the base of the Utrillas Formation, consisting of sandstones, claystones, siltstones, dolomitic siltstones, dolomitic marls, limestones and dolomitic limestones, with a mineralogy comprising calcite, dolomite, quartz, K-feldspar, lithic fragments and clay minerals (IGME, 1991).

The isotope $\delta^{18}O$ and $\delta^{2}H$ data available (IGME, 1982; 1994; Sanz and Yélamos, 1998; Pinuaga et al., 2004) indicate a clear meteoric origin. The tritium data available are also from the aforementioned works and they show the absence of tritium or levels close to the detection limit (≈ 1 TU) in the hottest springs. The most common interpretation for these results is that the thermal groundwaters have residence times longer than 50 years and that some of them are affected by minor mixing with shallow modern waters (Clark and Fritz, 1997).

3. METHODOLOGY

3.1. *Field sampling and analysis*

Six and nine springs were sampled in the Alhama and Jaraba thermal sites, respectively. Field sampling procedures and analytical methodology were mostly as described by Auqué et al. (2009). Briefly, at each sampling point, temperature, pH and conductivity were determined *in situ* and separated samples for anion and cation analysis were taken in 1N HCl pre-washed polyethylene bottles. Samples for cation analysis were filtered through 0.1 μm and acidified to pH less than 1 with ultrapure HNO_3. Anions were determined within 24 hours after collection. Total alkalinity was determined by titration with a Mettler titrator with an end-point electrode. Chloride and fluoride concentrations were determined by a selective ion analyser equipment, using the selective electrodes for chloride ORION 94-17B and fluoride ORION 94-09. Sulphate was determined by colorimetry using a modification of the Nemeth method (Nemeth, 1963). Potassium concentrations were analysed by Flame Photometry and aluminium concentrations were determined by Electrothermal Atomisation Atomic Absorption Spectrometry with Zeeman-effect background correction. Inductively Coupled Plasma-Atomic Emission Spectrometry was used for the analysis of the rest of the elements (Ca, Mg, Na, Li, and Si). The average analytical error was estimated <5% for alkalinity, chloride, fluoride, sulphate, potassium and aluminium, < 4% for Ca, Mg, Na and Si, and < 9% for Li.

The calculated charge balance error for the analyses reported, as calculated with the PHREEQC code (Parkhurst and Appelo, 2013), is below 5%.

3.2. *Methodology for geothermometrical calculations*

Various geothermometrical techniques are used in this work to ascertain the reservoir temperature in the Alhama-Jaraba system: classical and specific chemical geothermometers and geothermometrical modelling calculations. The integration of the results has helped to propose a temperature range in the

reservoir. The general features of these methodologies in their application to the system studied are detailed below.

3.2.1. Chemical geothermometers

Two main types of chemical geothermometers have been used (Table 1):

- Classical geothermometers, which include the dissolved silica geothermometer and several cationic geothermometers (Na-K, Na-K-Ca, Ca-K, K-Mg, Na-Li, Li and Mg-Li, some of them with several calibrations; Table 1). Most of these geothermometers have been proved to be very useful for estimating subsurface temperature in high temperature systems (>180 °C) where equilibria between aqueous solutions and minerals in the geothermal reservoirs are easily attained (e.g. Fournier, 1977, 1981; Fouillac and Michard, 1981; Arnorsson et al., 1983; Giggenbach et al., 1983; D'Amore et al., 1987; Nieva and Nieva, 1987; Giggenbach, 1988; Kharaka and Mariner, 1988; Chiodini et al., 1995; Mutlu and Gülec, 1998; Stefánsson and Arnórsson, 2000; Mariner et al., 2006; Sonney and Vuataz, 2010; Nicholson, 2012). However, in low to medium temperature hydrothermal systems (40-180 °C) hosted in carbonate-evaporitic rocks, these geothermometrical techniques encounter problems frequently related to the mineral assemblage expected to govern the water chemistry and to the attainment of equilibrium in the reservoir (Chiodini et al., 1995; Levet et al, 2002; Sonney and Vuataz, 2010). Nevertheless, some of these geothermometers have occasionally given good results in this type of system (e.g. Michard and Bastide, 1988; Minissale and Duchi, 1988; Pastorelli et al., 1999; Gökgöz and Tarcan, 2006; Mohammadi et al., 2010; Apollaro et al., 2012; Wang et al., 2015; Blasco et al., 2017; 2018) and, therefore, their performance will be assessed at the studied sites.

- Specific geothermometers, which were developed to be used in low-temperature carbonate-evaporitic systems, like the SO_4-F and the Ca-Mg geothermometers (Marini et al., 1986; Chiodini et al., 1995). The application of these geothermometers requires the existence of

anhydrite/gypsum – fluorite equilibrium, and calcite – dolomite equilibrium, respectively. Equilibrium with anhydrite or gypsum is easily attained in systems with evaporitic rocks in the host formations since these are the most common phases; however, the presence of fluorite is not so common in these environments (Chiodini et al., 1995).

The calcite–dolomite equilibrium can be represented by the following overall reaction and equilibrium equation (e.g. Appelo and Postma, 2005):

$$2CaCO_3 + Mg^{2+} \leftrightarrow CaMg(CO_3)_2 + Ca^{2+} \quad (1)$$

$$K = aCa^{2+} / aMg^{2+} = (K_{calcite})^2 / K_{dolomite} \quad (2)$$

where $a\mathrm{Ca}^{2+}/a\mathrm{Mg}^{2+}$ represents the activity ratio of dissolved calcium and magnesium in the target solution and $K_{calcite}$ and $K_{dolomite}$ represent the equilibrium constants for calcite and dolomite, respectively. As can be deduced from equation (2), one of its advantages is that the $a\mathrm{Ca}^{2+}/a\mathrm{Mg}^{2+}$ ratio mainly depends on temperature and it is not significantly influenced by variations in the CO_2 partial pressure or pH during the ascent of thermal waters towards spring conditions (Hyeong and Capuano, 2001). However, this geothermometer can also be problematic due to the uncertainties in the solubility of dolomite which make its use in geothermometry very difficult (e.g. Hyeong and Capuano, 2001; Palandri and Reed, 2001; Blasco et al., 2018). These uncertainties will be further evaluated.

Table 1. Calibrations used in this work for the different classical geothermometers. Geothermometrical functions provide the temperature values in degrees Celsius. The concentration units corresponding to the different expressions are also indicated (usually mg/L or mol/L).

Geothermometer	Authors of calibration	Expression	Units
SiO_2-quartz	Michard (1979)	$T = \frac{1322}{0.435 - log(SiO_2)} - 273.15$	mol/L
	Fournier and Potter (1982)	$T = \frac{1309}{5.19 - log(SiO_2)} - 273.15$	mg/L
Na-K	Giggenbach (1988)	$T = \frac{1390}{1.75 + \log(Na/K)} - 273.15$	mg/L
	Fournier (1979)	$T = \frac{1217}{1.483 + \log(Na/K)} - 273.15$	mg/L
Na-K-Ca[1]	Fournier and Truesdell (1973)	$T = \frac{1647}{\log(Na/K) + \beta\left[\log\left(\sqrt{Ca}/Na\right) + 2.06\right] + 2.47} - 273.15$	mg//L
Ca-K	Fournier and Truesdell (1973)[2]	$T = \frac{2920}{3.02 + \log\left(Ca/K^2\right)} - 273.15$	mol/L
	Michard (1990)	$T = \frac{3030}{3.94 + \log\left(Ca/K^2\right)} - 273.15$	mol/L
K-Mg	Giggenbach et al. (1983)	$T = \frac{4410}{13.95 - \log\left(K^2/Mg\right)} - 273.15$	mg/L
Na-Li	Fouillac and Michard, 1981	$T = \frac{1000}{0.33 + \log(Na/Li)} - 273.15$	mol/L
Li	Fouillac and Michard, 1981	$T = \frac{2258}{1.44 + \log(Li)} - 273.15$	mol/L
Mg-Li	Kharaka and Mariner, 1988	$T = \frac{2200}{5.47 + \log\left(\sqrt{Mg}/Li\right)} - 273.15$	mg/L
Ca-Mg[3]	Chiodini et al. (1995)	$T = \frac{979.8}{3.1170 - \log\left(Ca/Mg\right) + 0.07003 log \sum eq} - 273.15$	mol/L

[1] β=4/3 should be used if the temperature obtained is lower than 100 ºC; if the temperature obtained, using that value of β, is higher than 100 ºC, it should be recalculated considering β = 1/3. Mg-correction proposed by Fournier and Potter (1979) for the Na-K-Ca geothermometer cannot be applied to the studied springs, according to the criteria indicated by those authors.

[2]Derived from Fournier and Truesdell (1973) in Michard (1990).

[3] Σeq is the summation (in eq/L) of the major dissolved species.

3.2.2. Geothermometrical modelling

Geochemical modelling calculations provide a more generalised approach than the classical chemical geothermometry. This technique consists of simulating a process of a progressive water temperature increase to obtain a temperature range in which the saturation state of the waters with respect to a

selected mineral set (assumed to be present in the reservoir) simultaneously reaches equilibrium. When most of the minerals selected indicate about the same equilibrium temperature, the average temperature can be considered as the best estimate (e.g. Michard and Roekens, 1983; Reed and Spycher, 1984; D'Amore et al., 1987; Pang and Reed, 1998).

The geochemical modelling approach shows different advantages over the classical geothermometers. It helps to evaluate the secondary processes during the ascent of the thermal waters, such as 1) the extension of mineral reequilibrium reactions (Michard and Fouillac, 1980; Michard and Roekens, 1983; Michard et al., 1986), 2) the amount of lost gas and/or 3) the proportion of cold waters in mixtures (Pang and Reed, 1998; Palandri and Reed, 2001). It can also be advantageous to distinguish between equilibrated and non-equilibrated waters, as non-equilibrated waters result in a large range of calculated mineral equilibrium temperatures (e.g. Tole et al., 1993). However, this approach also has some uncertainties with respect to 1) the attainment of water-mineral equilibrium,2) the mineral solubility data input in calculations, and 3) the aluminium concentrations, which are low and can be easily affected by cooling during the ascent of thermal waters (Pang and Reed, 1998; Peiffer et al., 2014).

For the Alhama-Jaraba system, these geothermometrical modelling calculations have been carried out with the assistance of the PHREEQC geochemical code (version 3.4.0; Parkhurst and Appelo, 2013) and using two of the thermodynamic databases distributed with this version, WATEQ4F and LLNL, in order to perform a sensitivity analysis to the thermodynamic data.

Based on the mineralogy identified in the aquifer, the mineral phases selected for these calculations include: calcite, dolomite, quartz, gypsum/anhydrite and some aluminosilicates. Whereas the solubility constants for calcite, quartz, gypsum and anhydrite are fairly well known, there are some uncertainties related to the solubility dependence on temperature (K(T)) for the rest of the mineral phases. To evaluate their effects on the results obtained, the following procedures have been adopted:

- The solubility data for illite and smectites (beidellite, montmorillonite) are affected by potential problems such as their wide compositional variability, the variable degree of crystallinity, particle size effect, and some order/disorder phenomena (e.g. Merino and Ransom, 1982; Nordstrom et al., 1990; Palandri and Reed, 2001). However, illite has been used in geothermometrical calculations with some success (e.g. Pang and Reed, 1998 and Palandri and Reed, 2001), and, therefore, it is also used in this study to verify its performance and uncertainties. Also, the approach recommended by Helgeson et al. (1978) and Palandri and Reed (2001) has been followed and pyrophyllite and paragonite have been used as proxies for the whole set of clay minerals.

- The thermodynamic data for K-feldspar, kaolinite (two types with different crystallinity degrees: poorly crystalline and crystalline) and pyrophyllite from Michard et al. (1979) and Michard (1983) have been added to the WATEQ4F database for comparison with the data included in the LLNL.

- The solubility of dolomite is strongly affected by non-stoichiometry and order/disorder in Ca and Mg site occupancies (Helgeson et al., 1978; Carpenter, 1980; Reeder, 1990, 2000; Hyeong and Capuano, 2001) but experimental data on these effects do not exist. Therefore, in order to consider this uncertainty, we have tested the influence of several solubility values on the geothermometrical calculation results. For this purpose, the values included in the LLNL database, corresponding to fully-disordered and to fully-ordered dolomite were considered in the calculations together with the solubility value proposed for "dolomite" in the WATEQ4F database (Nordstrom et al., 1990; Dolomite_ W from now on), which represents a partially-ordered dolomite (Helgeson et al., 1978; Carpenter, 1980). Additionally, some natural dolomites with different degree of order/disorder have been included in the comparison: 1) the dolomite reported by Hyeong and Capuano (2001), from the Oligocene Frio Formation (Texas Gulf Coast) with an order of 11%

(Dolomite_H&C); 2) the dolomite considered by Busby et al. (1991) from the Carboniferous Madison Aquifer and an order of 23.5 % (Dolomite_B); 3) the dolomite used by Vespasiano et al. (2014) from the Triassic of Calabria (Italy) and an order of 22% (Dolomite_V); and 4) the dolomite reported by Blasco et al. (2018) from the Jurassic of the Cameros Basin (Spain) with an order of 18.4% (Dolomite_BL).

For comparative purposes, the solubility values at 25 °C and the K(T) function for the different mineral phases considered in the geothermometrical simulations are summarised in Table S1 (Supplementary Material).

4. RESULTS

4.1. *Hydrochemical characteristics of the thermal waters*

There are remarkable compositional differences among the springs studied. The thermal waters from Jaraba are mainly of Ca-Mg-HCO_3-type whilst in Alhama, the waters show a more distinct SO_4-Cl character with higher conductivity values and higher concentrations of Ca, Mg, Na, SO_4 and Cl (Table 2 and Figure 2). The alkalinity values are lower in Alhama than those determined in the Jaraba waters and the dissolved silica concentrations are similar in all waters although slightly lower in Jaraba waters.

The measured temperatures in the Alhama springs are always higher than 30 °C and their values are rather homogeneous (temperature variability smaller than 2.3 °C; Table 2) as it is also the case with the hydrochemical variability which is generally within the analytical error. The Jaraba springs, however, exhibit a larger compositional variability and temperature range (between 21 and 32 °C; Table 2) although the highest temperature is similar to those in Alhama. The combined variability of temperature and compositional characteristics in the Jaraba thermal waters has been attributed to mixing between deep thermal groundwaters and superficial and colder waters along the shallower

parts of the upflow towards the Jaraba springs (Tena et al., 1995; Auqué et al., 2009; Blasco et al., 2016).

Results of speciation-solubility calculations (Table 3) indicate that most of the springs studied in the Alhama and Jaraba sites are close to equilibrium or slightly oversaturated with respect to calcite and partially disordered dolomite (Dolomite_W or Dolomite_H&C; see above). The differences obtained in the saturation state of the waters with respect to calcite and dolomite are mainly related to the different extent of CO_2 outgassing along the shallowest parts of the flow paths (see Auqué et al., 2009 for further explanation and calculations on this issue). The highest values are found in sample ZA-45, from Alhama, which is the sample with the highest pH and a relative low log pCO_2 and, therefore, the one with the most intense outgassing.

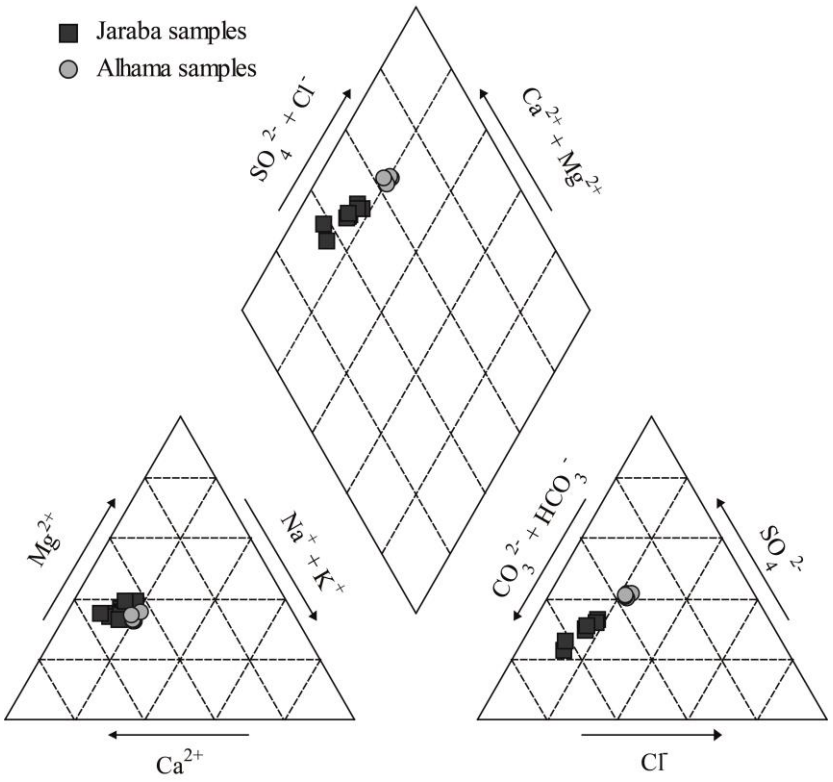

Figure 2. Representation of the composition of the water samples included in this study in a Piper–Hill diagram.

Table 2. General hydrochemistry of the Alhama-Jaraba thermal waters included in this study.

		Jaraba									Alhama de Aragón					
	Sample Number	**ZA-22**	**ZA-23**	**ZA-24**	**ZA-25**	**ZA-26**	**ZA-27**	**ZA-28**	**ZA-29**	**ZA-30**	**ZA-39**	**ZA-40**	**ZA-41**	**ZA-43**	**ZA-44**	**ZA-45**
	T (ºC)	26.6	27.3	27.2	21.0	29.4	32.0	31.8	26.1	21.8	30.1	31.9	32.4	30.2	31.6	30.7
	pH (field)	7.40	7.40	7.30	7.40	6.80	7.05	7.25	7.30	7.30	7.15	6.90	7.05	7.15	7.45	7.85
	Cond. (µS/cm)	865	864	850	755	890	910	905	859	745	1181	1154	1161	1152	1122	1122
mmol/L	HCO_3^-	4.73	4.72	4.72	4.92	4.65	4.62	4.68	4.68	4.81	4.38	4.47	4.39	4.49	4.47	4.58
	Cl^-	1.41	1.41	1.37	1.05	1.72	1.67	1.69	1.37	0.94	2.85	2.75	2.88	2.74	2.69	2.69
	SO_4^{2-}	1.32	1.37	1.28	0.88	1.58	1.54	1.5	1.36	1	2.6	2.56	2.6	2.44	2.44	2.52
	Ca^{2+}	2.31	2.31	2.30	2.09	2.10	2.41	2.39	2.10	2.27	3.05	2.97	3.08	3.06	2.73	2.98
	Mg^{2+}	1.74	1.67	1.61	1.35	1.92	1.68	1.55	1.76	1.44	2.08	2.07	2.13	2.17	2.21	2.22
	Na^+	1.4	1.4	1.3	1	1.7	1.5	1.5	1.3	0.8	2.6	2.6	2.6	2.6	2.6	2.3
	SiO_2	0.1512	0.1509	0.1492	0.1052	0.1501	0.1511	0.1389	0.1407	0.1257	0.1709	0.1674	0.1693	0.1286	0.1636	0.1663
µmol/L	K^+	30	30	25	25	30	30	30	30	15	40	40	40	40	40	70
	Li^+	5.0	5.0	5.0	5.0	5.0	6.1	6.1	6.1	1.0	12.0	9.9	9.9	9.9	6.1	7.9
	Sr^{2+}	1.5	3.0	1.9		4.0	4.5	4.5	1.9		10	9.5	10	9.5	9.5	9.5
	B	0.19						0.28			1.00	0.83	0.74	0.74	0.56	0.46
	Al						0.64		0.36		0.41	0.74	0.82			
	F^-	9.2	9.5	8.5	4.8	9.7	12.0	12.0	8.7	7.7	17.0	16.0	17.0	15.0	16.0	16.0

Table 3. Summary of results from speciation-solubility calculations in the Alhama-Jaraba thermal system. The calculations have been performed with the PHREEQC code (Parkhurst and Appelo, 2013) and the thermodynamic database WATEQ4F with some additional thermodynamic data included. Other results for aluminosilicate phases obtained using the LLNL thermodynamic database have been included for comparison.

	Jaraba									**Alhama de Aragón**					
Sample Number	**ZA-22**	**ZA-23**	**ZA-24**	**ZA-25**	**ZA-26**	**ZA-27**	**ZA-28**	**ZA-29**	**ZA-30**	**ZA-39**	**ZA-40**	**ZA-41**	**ZA-43**	**ZA-44**	**ZA-45**
Temperature (ºC)	26.6	27.3	27.2	21.	29.4	32.0	31.8	26.1	21.8	30.1	31.9	32.4	30.2	31.6	30.7
pH (field)	7.4	7.4	7.3	7.4	6.80	7.05	7.23	7.31	7.29	7.13	6.89	7.04	7.15	7.47	7.87
TIC (mmol/L)	5.06	5.05	5.15	5.30	6.04	5.36	5.16	5.10	5.30	4.94	5.47	5.07	5.04	4.70	4.60
log pCO_2	-1.96	-1.96	-1.86	-1.97	-1.34	-1.57	-1.76	-1.88	-1.87	-1.71	-1.45	-1.6	-1.72	-2.03	-2.44
Calcite	0.3	0.31	0.21	0.22	-0,32	0.02	0.21	0.16	0.15	0.11	-0.1	0.06	0.16	0.43	0.86
Dolomite_ H&C	0.54	0.55	0.33	0.30	-0.61	-0.02	0.31	0.31	0.12	0.14	-0.26	0.05	0.25	0.87	1.67
Dolomite_W	0.62	0.63	0.42	0.35	-0.52	0.08	0.41	0.39	0.18	0.24	-0.16	0.15	0.34	0.97	1.77
Dolomite dis	0.07	0.09	-0.12	-0.21	-1.05	-0.44	-0.11	-0.15	-0.39	-0.29	-0.68	-0.37	-0.19	0.44	1.24
Gypsum	-1.51	-1.48	-1.5	-1.67	-1.47	-1.44	-1.44	-1.51	-1.58	-1.18	-1.18	-1.17	-1.2	-1.25	-1.2
Anhydrite	-1.72	-1.69	-1.71	-1.9	-1.67	-1.63	-1.62	-1.73	-1.81	-1.37	-1.37	-1.35	-1.39	-1.44	-1.39
Halite	-7.4	-7.4	-7.43	-7.67	-7.24	-7.3	-7.3	-7.43	-7.82	-6.85	-6.85	-6.84	-6.87	-6.87	-6.92
Fluorite	-2.54	-2.52	-2.61	-3.04	-2.58	-2.37	-2.35	-2.62	-2.6	-2.	-2.08	-2.02	-2.1	-2.11	-2.07
Chalcedony	-0.29	-0.3	-0.3	-0.36	-0.32	-0.35	-0.38	-0.32	-0.3	-0.28	-0.3	-0.3	-0.39	-0.32	-0.29
Quartz	0.13	0.12	0.12	0.08	0.09	0.06	0.03	0.11	0.14	0.14	0.11	0.11	0.02	0.09	0.12
Kaolinite	---	---	---	---	---	2.81	---	2.42	---	2.57	3.31	3.06	---	---	---
Kaolinite (crys)[1]	---	---	---	---	---	4.05	---	3.68	---	3.81	4.56	4.31	---	---	---
Kaolinite (poor crys)[1]	---	---	---	---	---	3.28	---	2.96	---	3.06	3.79	3.53	---	---	---
Kaolinite[2]	---	---	---	---	---	3.85	---	3.50	---	3.62	4.33	4.11	---	---	---
K-Feldspar[1]	---	---	---	---	---	-0.24	---	-0.11	---	-0.01	0.10	0.11	---	---	---
Albite[1]	---	---	---	---	---	-1.01	---	-0.97	---	-0.67	-0.56	-0.54	---	---	---
Albite[2]	---	---	---	---	---	-0.96	---	-0.90	---	-0.62	-0.52	-0.49	---	---	---
Paragonite[2]	---	---	---	---	---	2.83	---	2.35	---	2.75	3.62	3.46	---	---	---
Pyrophyllite[1]	---	---	---	---	---	2.12	---	1.83	---	2.04	2.75	2.48	---	---	---
Pyrophyllite[2]	---	---	---	---	---	2.43	---	2.19	---	2.36	3.02	2.79	---	---	---

[1]Thermodynamic data from Michard et al. (1979) and Michard (1983).

[2]LLNL thermodynamic database distributed with PHREEQC.

The studied waters are undersaturated with respect to all silica minerals, except quartz, and also with respect to gypsum, anhydrite, fluorite, halite and albite and slightly undersaturated or near equilibrium with respect to K-feldspar (Table 3 and Figure 3). They are, however, clearly oversaturated with respect to the rest of the aluminosilicates potentially present in the deep reservoir, kaolinite, illite, paragonite and pyrophyllite. As mentioned above, knowing the uncertainties associated to the thermodynamic data for the aluminosilicates, these results have been checked using different thermodynamic data (Table 3 and Figure 3) and the variations found do not change the over- or undersaturation results commented above significantly.

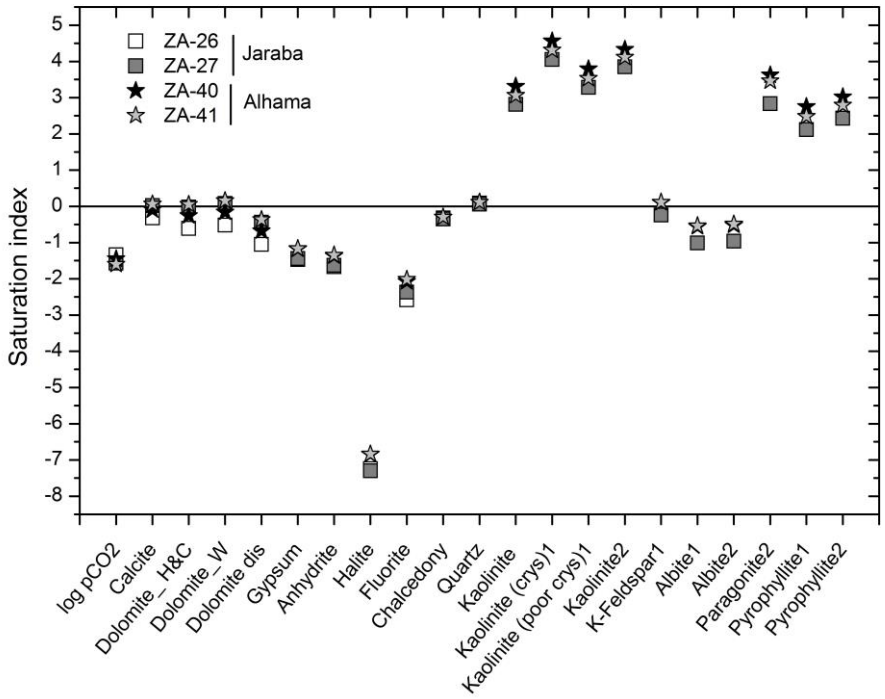

Figure 3. Computed saturation indices for the mineral phases considered. Results shown are for two samples from each site, those with lower pH and higher temperature and, therefore, considered most suitable for geothermometrical calculations. The calculations have been performed with the PHREEQC code (Parkhurst and Appelo, 2013) and the thermodynamic database WATEQ4F with some additional thermodynamic data included. Other results for aluminosilicate phases obtained using the LLNL thermodynamic database have been included for comparison. The thermodynamic data for mineral phases marked with the number 1 are from Michard et al. (1979) and Michard (1983), and those with the number 2 from the LLNL database.

Based on the combination of ion-ion plots, speciation-solubility calculations, mass-balance and reaction-path modelling, Auqué et al. (2009) suggested that the most important geochemical processes determining the geochemical evolution, along one of the possible flow directions from the Solorio recharge zone through Mochales, Jaraba and Alhama groundwaters (see Figure 1), are: 1) halite dissolution (note the 1:1 relation for Cl and Na contents both in the Jaraba and Alhama thermal waters; Table 2) and 2) dedolomitisation (dolomite dissolution and concomitant calcite precipitation triggered by gypsum/anhydrite dissolution).

The extent of the halite and gypsum/anhydrite dissolution processes seems to be constrained only by the water-rock interaction time and/or by the availability of these minerals in the system. However, the dolomite dissolution and calcite precipitation (dedolomitisation) appear to evolve through partial equilibrium or near partial equilibrium between calcite and dolomite along the entire flow path and all over the system. This situation is consistent with the very similar Mg/Ca ratio, around 0.7, found in the Jaraba and Alhama thermal waters (considering the ZA-27 sample from Jaraba as it is not affected by the mixing process) which is indicative of the existence of a calcite-dolomite equilibrium (or near equilibrium) at similar temperatures in the aquifer. A more detailed description of the hydrogeochemistry and evolution of the Alhama-Jaraba thermal system can be found in Auqué et al. (2009).

4.2. *Geothermometrical calculations*

4.2.1. Chemical geothermometers

Table 4 and Figure 4 summarise the results obtained with the various chemical geothermometers. Prior to the application of the classical cation geothermometers, the main cation concentrations of the water samples were plotted in the classical Giggenbach ternary Na-K-Mg diagram (Giggenbach, 1988) in order to check their applicability in this system. All the samples fall in the field of immature waters (almost in the Mg vertex; see Figure S1 in the Supplementary material) indicating that they have not

attained equilibrium with respect to the phases on which the classical cation geothermometers are based and, therefore, making their use unsuitable for this system. The spring waters from this system are undersaturated with respect to all silica phases except quartz and therefore, this geothermometer is the only silica geothermometer that provides temperatures higher than spring temperatures, with maximum values around 40 °C for the Alhama waters and 37 °C for the Jaraba ones. The rest of the cation geothermometers indicate excessively high or low temperatures, as expected from the application of the Giggenbach diagram: high in the case of the Na-K geothermometer and lower than the temperatures measured under spring conditions, in the case of the K-Mg geothermometer (Table 4 and Figure 4). The Na-K-Ca geothermometer also provides too low temperatures. The temperatures obtained with the Ca-K geothermometer depend on the calibration considered (Table 4 and Figure 4): the calibration proposed by Fournier and Truesdell (1973) provides reasonable temperatures about 40 ºC, whilst the calibration from Michard (1990) estimates a temperature lower than the spring temperature, about 20 ºC. This situation, along with the fact that this Ca-K geothermometer is deduced from the Na-K-Ca geothermometer, whose results are also inconsistent, suggests that the Ca-K geothermometer`s results are affected by important uncertainties and therefore, they will not be considered in this study. Finally, the Mg-Li geothermometer provides temperatures below the spring temperature and, although the other two lithium geothermometers (Na-Li and Li) provide higher temperatures (62 - 108 °C), their results are uncertain (e.g. D'Amore et al., 1987) as they were not specifically calibrated for waters with Li concentrations below 1 ppm (which is the case of the Alhama-Jaraba waters).

It is not surprising that the application of most of these cation geothermometers leads to erroneous results, but what is interesting is that in other similar carbonate-evaporitic systems, where some detrital components are also present, these classical cation geothermometers have provided reliable results (e.g. Fernández et al., 1988; Michard and Bastide, 1988; Pastorelli et al., 1999; Gökgöz and Tarcan, 2006; Mohammadi et al., 2010; Apollaro et al., 2012; Wang et al., 2015; Blasco et al., 2017; 2018). This different performance will be discussed later.

The Ca-Mg geothermometer proposed by Chiodini et al. (1995), based on a disordered dolomite, provides temperatures ranging from 61 to 75 ºC, slightly higher than the temperatures obtained with the SiO_2-quartz geothermometer. However, one has to take into account that this geothermometer is based on the simultaneous equilibrium calcite-dolomite and therefore, the results are strongly affected by the solubilities of both minerals, and as the solubility of calcite is fairly well-constrained, the main effects come from the uncertainties in the dolomite solubility. There is a wide range of proposed solubilities for dolomite depending mainly on the degree of crystallographic order assumed for this phase and as a result this can lead to different temperature results depending on the order degree of the dolomite considered. This issue will be addressed further in this study.

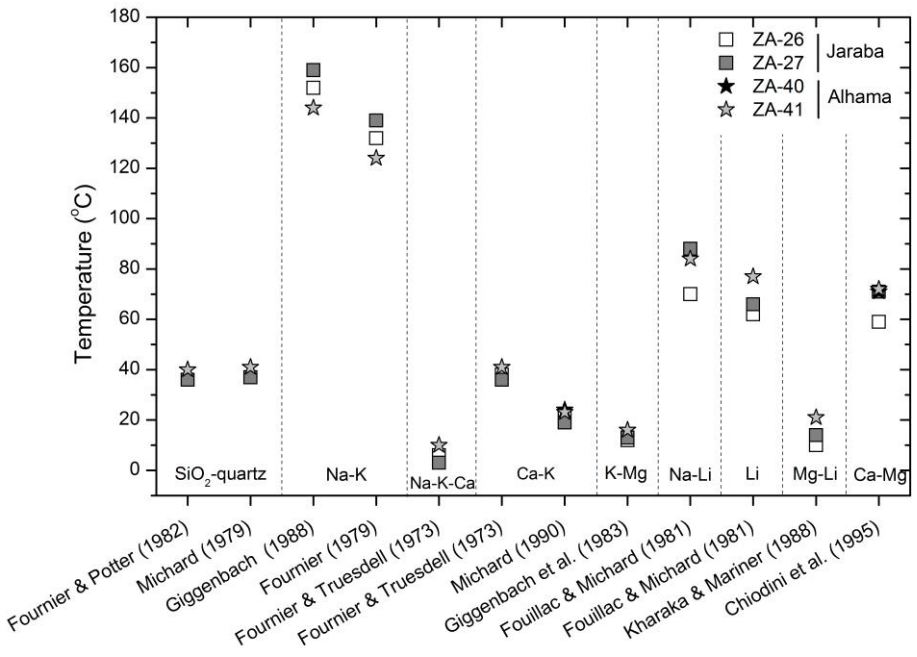

Figure 4. Results obtained with some classical chemical geothermometers. Two samples from each site have been chosen. These samples are the ones with lower pH and higher temperature and, therefore, considered less affected by degassing and/or mixing and thus most suitable for geothermometrical calculations (see text).

With respect to the use of the geothermometers developed for this type of system (SO_4-F and Ca-Mg; Marini et al., 1986; Chiodini et al., 1995) some problems have also been found. The SO_4-F

394 geothermometer cannot be used in the studied system as it is only applicable in the cases where
395 equilibria anhydrite-fluorite or gypsum-fluorite are fulfilled, which is not the case for the
396 Alhama-Jaraba system neither under spring conditions nor in the deep aquifer (see below).
397

Table 4. Temperature results (in °C) obtained with some classical chemical geothermometers for the Alhama-Jaraba thermal waters. Shadowed rows correspond to the most suitable samples from Alhama and Jaraba sites (highest temperatures and lowest pH values) for the geothermometrical calculations (ZA-26 and ZA-27 for Jaraba; ZA-40 and ZA-41 for Alhama).

		Jaraba									Alhama					
		ZA-22	**ZA-23**	**ZA-24**	**ZA-25**	**ZA-26**	**ZA-27**	**ZA-28**	**ZA-29**	**ZA-30**	**ZA-39**	**ZA-40**	**ZA-41**	**ZA-43**	**ZA-44**	**ZA-45**
Spring Temp. (°C)		27	27	27	21	29	32	32	26	22	30	32	32	30	32	31
SiO_2−quartz	Fournier & Potter (1982)	36	36	36	26	36	36	34	34	31	40	40	40	31	38	40
	Michard (1979)	37	37	37	28	37	37	35	35	33	41	41	41	33	39	41
Na−K	Giggenbach (1988)	163	163	156	172	152	159	159	167	159	144	144	144	144	144	185
	Fournier (1979)	143	143	137	153	132	139	139	148	139	124	124	124	124	124	166
Na−K−Ca	Fournier & Truesdell (1973)	3	3	-1	-1	6	3	3	4	-14	10	10	10	10	11	21
Ca-K	Fournier and Truesdell (1973)	37	37	31	33	38	36	36	38	18	41	41	41	41	43	58
	Michard (1990)	20	20	15	16	21	19	19	21	4	24	24	23	23	25	38
K−Mg	Giggenbach et al. (1983)	13	13	10	11	12	13	14	12	3	16	16	16	15	15	25
Na-Li	Fouillac & Michard (1981)	81	81	85	100	70	88	88	96	34	95	84	84	84	59	78
Li	Fouillac & Michard (1981)	62	62	62	62	62	66	66	66	30	82	77	77	77	66	72
Mg-Li	Kharaka & Mariner (1988)	11	11	12	13	10	14	15	14	-11	24	21	21	20	12	17
Ca-Mg	Chiodini et al. (1995)	69	69	72	75	59	71	78	61	80	71	71	72	70	63	68

4.2.2. Geothermometrical modelling results

As mentioned above, this type of modelling consists of simulating a process of progressive water temperature increase to obtain the temperature range at which a set of minerals (assumed to be present in the reservoir in equilibrium with the waters) simultaneously reaches equilibrium. One of the main difficulties when reconstructing the equilibrium situation at depth through heating simulations is related to the possible hydrogeochemical modifications by secondary processes that may have affected the chemistry of the waters during their ascent to the surface (Pang and Reed, 1998; Peiffer et al., 2014). That is why the selection of the spring water with which the simulations are going to be performed is crucial.

In previous works, mixing with cooler and shallower waters and CO_2 outgassing have been reported as the main secondary processes affecting the hydrogeochemistry of the system studied (see Tena et al., 1995, Auqué et al., 2009 and Blasco et al., 2016 for details). In order to minimise their effects in the modelling, the water samples selected for the geothermometrical simulations are those with the highest temperatures (less probability of have been affected by mixing) and with the lowest pH values (less probability of havingbeen affected by CO_2 outgassing). The two samples are:

- sample ZA-40 (Alhama) which almost fulfils both conditions, the lowest pH of the site and a spring temperature only 0.5 °C lower than the maximum measured temperature spring, ZA-41 (Table 2); and
- sample ZA-27 (Jaraba) with the highest measured spring temperature and not affected by mixing (evident process in the Jaraba set; Tena et al., 1995; Pinuaga et al., 2004; Auqué et al., 2009, Blasco et al., 2016) as the chemical composition is very constant with time and it belongs to the group of waters without tritium in the Jaraba group (Tena et al., 1995; Blasco et al., 2016). The problem with this sample is that the pH value (pH=7.05; Table 2) is not the lowest among the Jaraba waters probably due to CO_2 outgassing. Therefore, in order to correct the possible effects of this, a theoretical addition of CO_2 (as recommended by Pang and Reed,

1998 and Palandri and Reed, 2001) has been simulated with PHREEQC up to the point at which the lowest pH value measured in the area is obtained (pH = 6.80 in sample ZA-26, adding 0.6 mmol/L of CO_2).

The results of the geothermometrical simulations with the PHREEQC geochemical code, using the LLNL and WATEQ4F thermodynamic databases are shown in Figure 5 and Table 5. The general results indicate that these thermal waters are highly undersaturated with respect to albite, gypsum, anhydrite and fluorite not only under spring conditions (as seen above) but within the whole temperature range considered in the simulations.

Quartz equilibrium is reached at rather similar temperatures (37-40 °C) in both waters (Figure 5 and Table 5) and coincides with the equilibrium for calcite and dolomite in Alhama, especially when considering the partially-ordered dolomite from Hyeong and Capuano (2001; Dolomite _H&C). Average equilibrium temperatures between the two databases with respect to calcite and dolomite are 41.5 ± 1.5 °C in Alhama and 50.5 ± 2.5 °C in Jaraba when considering the partially-ordered Dolomite_H&C only. The range in the equilibrium temperatures is increased if fully-disordered dolomite is considered (48 ± 8 °C for Alhama and 56 ± 8 °C for the Jaraba thermal waters) although the temperature provided by this phase, which is more soluble than the others, should be considered as a maximum temperature (Blasco et al., 2018). As a conclusion, it can be said that the good convergence among the temperatures estimated using quartz, calcite and dolomite equilibria (unaffected by possible CO_2 outgassing problems in the case of quartz, but affected for the carbonates) confirm that the samples selected for the geothermometrical simulations are not significantly affected by CO_2 outgassing during the rise of these thermal waters to the surface (e.g. Pang and Reed, 1998).

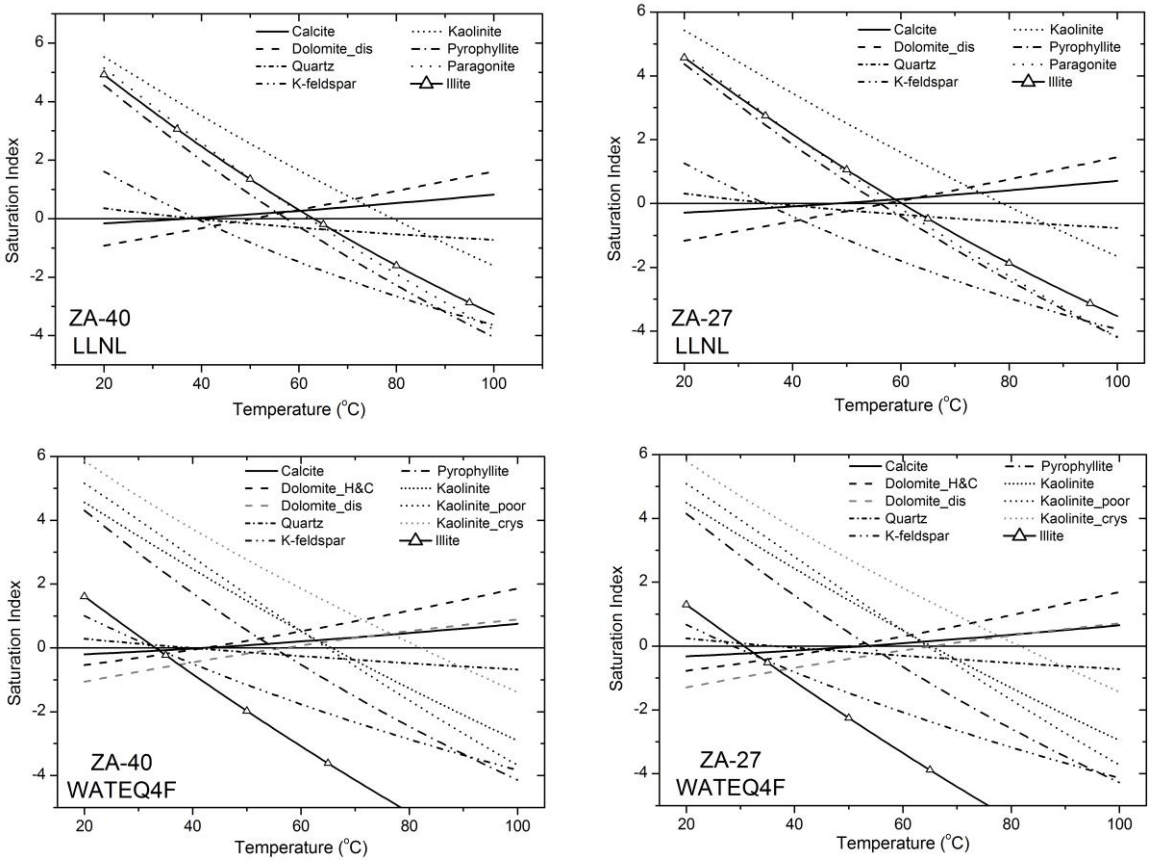

448

449 **Figure 5**. Evolution with temperature of the saturation indices of the minerals presumed to be in
450 equilibrium with the waters in the reservoir. The waters shown here correspond to sample ZA-27 from
451 Jaraba and ZA-40 from Alhama. The calculations have been performed with two different
452 thermodynamic databases, LLNL (upper two plots) with the original data and WATEQ4F (lower
453 plots) with additional data for many of the minerals of interest: the thermodynamic data for the
454 partially ordered dolomite were taken from Hyeong and Capuano (2001; Dolomite_H&C) and the data
455 for crystalline kaolinite (Kaolinite_crys), poorly crystalline kaolinite (Kaolinite_poor), K-feldspar and
456 pyrophyllite were taken from Michard (1983). Dolomite_dis represents in both cases the disordered
457 dolomite included in each database.

458

Table 5. Equilibrium temperatures (in °C) for the minerals considered in the geothermometrical simulations for the selected samples from Alhama and Jaraba thermal waters. Results with the WATEQ4F and LLNL thermodynamics databases are shown.

	ZA-27 (Jaraba)		ZA-40 (Alhama)	
	WATEQ4F	LLNL	WATEQ4F	LLNL
Calcite	53	48	43	40
Dolomite (dis)	64	57	56	51
Dolomite_ H&C	51	----	42	----
Quartz	37	37	40	40
K-Feldspar	29[1]	35	33[1]	39
Kaolinite	65	79	63	79
Kaolinite (poor crys)	64[1]	----	65[1]	----
Kaolinite (crys)	81[1]	----	82[1]	----
Illite	31	60	44	63
Pyrophyllite	54[1]	56	56[1]	57
Paragonite	----	59	----	62

[1] Using the thermodynamic data from Michard et al. (1979) and Michard (1983).

To verify the previous determinations, the modelling has been repeated for another sample presumably only affected by CO_2 outgassing, sample ZA-39 but reconstructing the characteristics of the waters at depth before the CO_2 loss (Palandri and Reed, 2001; Pang and Reed, 1998). For this purpose, about 0.45 mmol/L of CO_2 have been added to the ZA-39 sample, giving a pH value identical to that in sample ZA-40 (6.90). The equilibrium temperatures obtained for the mineral phases are almost the same as those presented above for sample ZA-40, without CO_2 outgassing, which suggests that the CO_2 outgassing is the main process affecting the waters at this site and that the effects of other secondary processes such as dissolution/precipitation are negligible, if any.

With regard to the results obtained with the aluminosilicate minerals included in the calculations (K-feldspar, pyrophyllite, paragonite, illite and kaolinite), the temperature values depend strongly on the thermodynamic data used.

1. For K-feldspar, the temperature ranges between 13 and 39 °C depending on the thermodynamic data and the sample considered (Table 5 and Figure 5). K-feldspar solubility depends on the range of composition of the alkali-feldspar solid solutions and on the degree of

Al-Si order/disorder (Stefánsson and Arnórsson, 2000). These uncertainties make it very difficult to figure out the possible participation of this phase at equilibrium at depth and, therefore, these results will be disregarded.

2. The reservoir temperature values indicated by the equilibrium of illite, pyrophyllite and paragonite are in all cases between 40 and 62 °C (except in the case of the temperature obtained with illite and WATEQ4F in the Jaraba sample which is only 31ºC), in good agreement with the results obtained for calcite, dolomite and quartz.

3. Finally, the equilibrium temperature for kaolinite depends on the assumed degree of crystallinity for this mineral (Michard et al., 1979; Sanjuan et al., 1988; Nordstrom et al., 1990), ranging from 49 to 82 °C. The lowest values correspond to a poorly crystalline kaolinite and the highest temperatures to more crystalline varieties (Table 5). This implies that, if kaolinite participates in the equilibrium assemblage of the Alhama-Jaraba thermal waters, which suggests temperatures mostly lower than 60 °C, it will be a poorly-crystalline phase (as also found in other low-temperature carbonate aquifers; Michard and Bastide, 1988).

These results are also affected by the problems, associated with the analytical determination of low aluminium concentrations and/or the formation of colloids and the possible precipitation of Al-bearing phases during the ascent of the thermal waters (Pang and Reed, 1998: Peiffer et al., 2014). To evaluate the potential effects of these uncertainties the FixAl method proposed by Pang and Reed (1998) has been applied and K-feldspar equilibrium was imposed in the geothermometrical modelling (Figure S2 in Supplementary Material). The results indicate that in doing so, Al concentrations in the waters would be higher than the measured ones and that there is a lack of convergence of the SI values for the rest of the aluminosilicate phases, which is worse than the previous results (compare the results in Figure 5 and Figure S2). Similar situations have been obtained when imposing equilibria with other aluminosilicate phases (e.g. kaolinite, muscovite; Pang and Reed, 1998) in the calculations (not shown), suggesting that dissolved aluminium in the waters studied is not meaningfully affected by

502 secondary processes (e.g. reequilibria with respect to Al-bearing phases) during the ascent of the
503 thermal waters.

504 Overall, a value of 51 ± 14 °C is indicated from the equilibria with respect to quartz, calcite, dolomite
505 (Dolomite_H&C, partially disordered; Hyeong and Capuano, 2001), pyrophyllite, paragonite and low
506 crystalline kaolinite, as the most probable temperature range at depth in the Alhama-Jaraba thermal
507 system. This range takes into account the thermodynamic uncertainties for the key minerals and
508 encloses the temperature values deduced by the quartz geothermometer.

509 ## 5. DISCUSSION

510 The combination of different geothermometrical approaches and sensitivity analysis to thermodynamic
511 data has allowed defining a probable temperature range for the Alhama-Jaraba thermal waters in the
512 aquifer at depth.

513 The results presented here support the expected unsuitability of most cationic geothermometers for the
514 estimation of the reservoir temperatures in low temperature environments and/or in carbonate-
515 evaporitic reservoirs (Henley et al., 1984; D'Amore et al., 1987; Minissale and Duchi, 1988; Mutlu
516 and Gülec, 1998; López-Chicano, 2001; Levet et al., 2002; Karimi and Moore, 2008; Sonney and
517 Vuataz, 2010). The application of these classical geothermometers to the Alhama-Jaraba thermal
518 waters leads to temperatures either too high (compared with the combined results of other
519 methodologies) or too low (below spring temperature). The question that arises here is why these
520 geothermometers have provided coherent results in other similar low temperature systems hosted in
521 carbonate–evaporitic rocks and not in this particular one. Blasco et al. (2017, 2018) have studied some
522 examples of this situation and they indicate that the good results found in those systems are
523 conditioned by the existence of detrital rocks in the carbonate–evaporitic reservoir, allowing the
524 waters to reach equilibrium with respect to the phases on which these geothermometers are based. In
525 this case, their unsuitability, despite the presence of some detrital formations in the aquifer, seems to

526 be related to the shorter residence time of the waters or the less homogeneous distribution of this
527 specific mineralogy.

528 The SO_4-F chemical geothermometer, based on the anhydrite–fluorite equilibria, was developed
529 specifically for carbonate–evaporitic systems; however, it is not always applicable in them as fluorite
530 is not a common mineral in these aquifers (e.g. Blasco et al. 2017; 2018). This is also the situation in
531 the Alhama–Jaraba system and therefore this geothermometer cannot be applied here. Additionally,
532 dispersed anhydrite has been identified in the aquifer studied although in a clear undersaturation state
533 that produces its dissolution and the associated dedolomitisation process that controls the geochemical
534 evolution of these thermal waters (Auqué et al., 2009). The disequilibrium of the waters with respect
535 to anhydrite prevents the use of one of the most reliable equilibria in the geothermometrical modelling
536 of this type of system, which is the equilibrium quartz/chalcedony–anhydrite (see below).

537 The results obtained with the Ca-Mg geothermometer (Marini et al., 1986; Chiodini et al., 1995), also
538 developed for carbonate–evaporitic rocks, range between 63 and 78 °C, but the uncertainties related to
539 the crystallinity and solubility of dolomite prevent it from obtaining a unequivocal estimation of the
540 reservoir temperature. As already explained, this is one of the main difficulties in the
541 geothermometrical calculations developed for this type of carbonate system and it constitutes a major
542 limitation for their application to natural systems. In order to avoid these uncertainties, various
543 dolomites have been used here in the geothermometrical modelling and the most consistent result (i.e.
544 the best convergence between calcite and dolomite towards SI=0) has been obtained considering the
545 dolomite provided by Hyeong and Capuano (2001), which indicates that the dolomite present in the
546 reservoir of the Alhama-Jaraba thermal waters should be of a similar order as Dolomite (H&C), which
547 is 11%.

548 To explore the importance of the order of dolomite on the classical geothermometrical results, log
549 ($a\mathrm{Ca}^{2+}/a\mathrm{Mg}^{2+}$) values have been calculated from equation (2) for the different dolomites included in
550 the WATEQ4F and LLNL databases, and also for other dolomites present in natural systems, at

different temperatures. As shown in Figure 6, there is a wide variability field of log (aCa^{2+}/aMg^{2+}) values (and, therefore, of possible estimated temperatures) depending on the type of dolomite assumed in the calculations. The average log (aCa^{2+}/aMg^{2+}) values calculated with PHREEQC are very similar for Alhama and Jaraba thermal waters (around 0.16; when considering the sample without mixing in Jaraba) and this value corresponds to reservoir temperatures about 77 °C when considering the fully-disordered dolomite (Figure 6). The presence of this type of dolomite is quite improbable in old rocks from the Jurassic-Cretaceous, but, in any case, this temperature can be considered as a maximum estimate (Blasco et. al., 2018). On the other hand, the calculations indicate the impossibility of occurrence of a fully-ordered dolomite in equilibrium with the waters studied (which would imply values of log (aCa^{2+}/aMg^{2+}) above 1.2; see Figure 6). In agreement with the results of the geothermometrical modelling, the most consistent result is the one obtained when this calculation is carried out considering the partially ordered dolomite with an order degree of 11% (dolomite_H&C). Finally, following the methodology suggested by Blasco et al. (2018) to deal with these uncertainties, the approximate order degree of the dolomite present in this system was calculated considering samples ZA-27, from Jaraba, and ZA-40, from Alhama. The order degree obtained for the dolomite in the reservoir of this thermal system is similar for both samples: 11.3% in the case of Jaraba and 14.7 % in the case of Alhama, as expected close to the value for the dolomite studied by Hyeong and Capuano (2001).

Quartz equilibrium in the geothermometrical simulations (and quartz geothermometer results) provides reasonable values, in the lower range of the estimated temperature (51 ± 14 °C).

Quartz (or chalcedony) – anhydrite equilibrium has been shown to be a reliable indication of the reservoir temperature (e.g. Pastorelli et al. 1999; Levet et al., 2002; Alçiçek et al., 2016; 2017; Blasco et al., 2017; 2018). Unfortunately, as mentioned above, this equilibrium is not applicable to this system because anhydrite equilibrium is not reached.

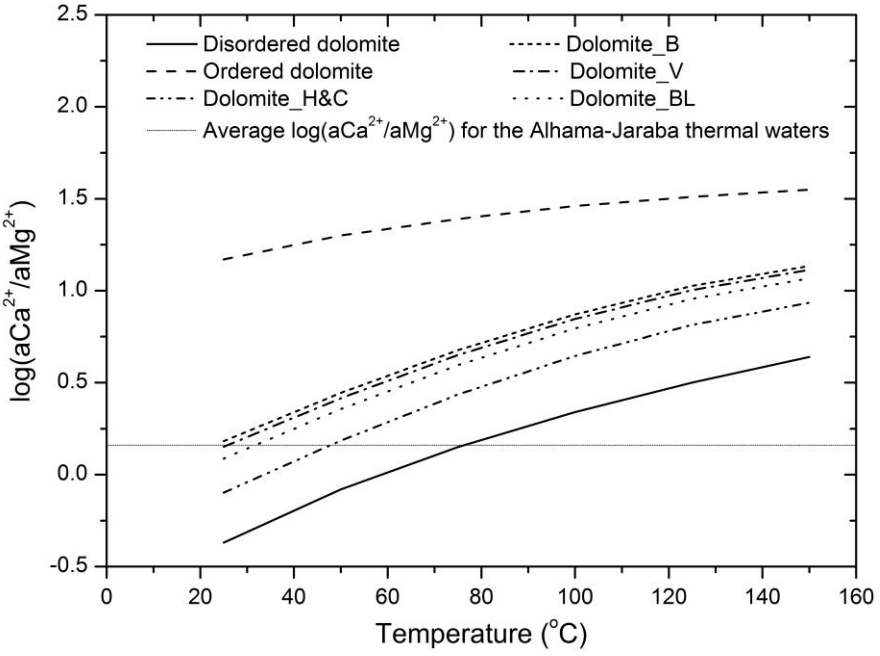

575

576 **Figure 6.** Log (aCa^{2+}/aMg^{2+}) vs. temperature plot for the calcite–dolomite equilibrium using different
577 dolomites, from 25 to 150 °C. The equilibria with respect to calcite and fully-disordered dolomite and
578 with respect to calcite and fully-ordered dolomite, have been calculated with the thermodynamic data
579 in the LLNL database. The equilibria with respect to calcite and some partially ordered dolomites
580 present in natural systems are also shown (see text) The log (aCa^{2+}/aMg^{2+}) average value (0.146)
581 calculated with PHREEQC for the Jaraba and Alhama thermal waters is also represented as a
582 horizontal grey line.

583 For other key minerals (K-feldspar and aluminosilicate phases), the estimated reservoir temperature
584 range in geothermometrical simulations depends strongly on the thermodynamic data selected and Al
585 concentration. However, using reasonable solubility "end-members" for these minerals (covering
586 differences due to the degree of crystallinity, particle size effects or the order/disorder phenomena), a
587 relatively narrow temperature range of ± 20 °C can be obtained, in agreement with one of the scarce
588 earlier uncertainty estimations for geothermometrical modelling, carried out by Tole et al. (1993).

589 Taking into account all the geothermometrical techniques applied in this study and the usual
590 uncertainties considered in the temperatures obtained with classical geothermometers (± 5 to ± 10 °C

591 and may be greater than 20ºC; Fournier, 1982), or geochemical modelling (± 20 °C; Tole et al., 1993),
592 the temperature estimate of 51 ± 14 °C for the Alhama-Jaraba thermal waters can be considered quite
593 probable. This common temperature range at depth for the Alhama and Jaraba thermal waters would
594 be in agreement with the idea that their origin is from the same aquifer.

595 Furthermore, the results of the studies carried out in the context of the ALGECO2 project (IGME,
596 2010) in the area of the Almazán Basin, indicate that the carbonate aquifer reaches a depth of about
597 1200 m. The geothermal gradient for the Almazán Basin is about 30 °C/Km (Fernández et al., 1998)
598 and, thus, considering an average air temperature of about 14 - 15 °C in this area (López et al., 2007),
599 the estimated temperature at these depths would be 52 °C, in close agreement with the average
600 temperature obtained from the combined techniques used in this study.

601 ## 6. CONCLUSIONS

602 The waters of the low temperature Alhama-Jaraba geothermal system, hosted in carbonate rocks and
603 one of the largest naturally flowing thermal systems in Europe, have been characterised in this study,
604 and various chemical geothermometrical techniques have been tested.

605 The thermal waters in the Jaraba springs are of Ca-Mg-HCO_3-type whilst they are more SO_4-Cl type in
606 Alhama. The range of emerging temperatures in the Alhama springs is quite narrow, between 30 and
607 32.4 ºC, while in Jaraba the temperatures range between 21 and 32 ºC, due to the effects of mixing
608 with shallower and cooler waters. Variable CO_2-outgasssing processes affect different springs at both
609 sites, promoting changes in the pH values of the waters. In summary, the Alhama-Jaraba system, as a
610 whole, brings together almost all drawbacks and possible difficulties for the application of the
611 geothermometrical methods in this type of low temperature geothermal system: problems related to
612 the existence of secondary processes during the ascent of the thermal waters and problems related to
613 the effective mineral equilibria in the reservoir at low temperatures.

614 The effects of the secondary processes identified can be minimised with 1) a careful selection of the
615 adequate samples for the geothermometrical calculations (e.g. discarding those samples affected by
616 mixing) and/or 2) using the reconstruction methodologies available when applying the
617 multicomponent geothermometrical methods (e.g. adding CO_2 to reverse the effects of CO_2-outgassing
618 during the ascent of the thermal waters).

619 The mineralogical/lithological characteristics of the aquifer importantly constrain the mineral
620 equilibria at depth and, therefore, the results obtained with the classical geothermometers or with the
621 multicomponent geothermometry. Cation geothermometers have been successfully used in some
622 carbonate-evaporitic geothermal systems with presence of detritial rocks in the aquifer. These detrital
623 rocks are also present in the Alhama-Jaraba system but the lower residence times, the lower
624 temperature at depth and/or the more disperse distribution of siliciclastic materials in the aquifer
625 prevent the waters from attaining the mineral equilibria on which these geothermometers are based
626 (e.g. albite and K-feldspar). This has also been confirmed in the results of the geothermometrical
627 modelling.

628 The aquifer studied is dominated by carbonates with only a slight evaporitic character reflected by the
629 low abundance of gypsum/anhydrite in the rocks and by the disequilibrium of the waters with respect
630 to these phases. Due to this disequilibrium, the SO_4–F geothermometer (specifically developed for
631 carbonate-evaporitic geothermal systems) and the equilibrium quartz (or chalcedony)–anhydrite (one
632 of the most reliable equilibria in the geothermometrical modelling), cannot be used for this system.

633 Therefore, the only possible mineral equilibria available for the geothermometrical calculations in
634 systems like the one presented here are silica polymorphs, calcite, dolomite and clay minerals. After
635 evaluating the results obtained with different silica phases, the SiO_2-quartz geothermometer appears to
636 provide consistent results in the system studied. The evaluation of the dolomite and clay mineral
637 equilibria, however, shows important uncertainties in the solubility values available related to degree
638 of crystallinity, particle size effects and/or the order/disorder phenomena.

Although the waters are in equilibrium with respect to calcite and dolomite, the uncertainties associated with the order degree of dolomite affect the Ca-Mg geothermometer and the evaluation of this equilibrium by geothermometrical modelling. To deal with these uncertainties a possible strategy is the one applied in this paper, consisting of evaluating the results obtained with different dolomites (with the Ca-Mg geothermometer and the geochemical modelling).

Finally, clay mineral equilibria in the geothermometrical modelling provide consistent results within a reasonable uncertainty range, as long as proper sensitivity analysis is performed in order to evaluate the effects of the thermodynamic data selected.

By applying all these methods, the reservoir temperature for the Alhama-Jaraba system has been established to be 51 ± 14 ºC, with waters in equilibrium with quartz, calcite, partially-ordered dolomite and some aluminosilicate phases. This temperature is in close agreement with that deduced from the results of geophysical studies in the area.

7. ACKNOWLEDGEMENTS

M. Blasco has worked on this study thanks to a scholarship from the Ministry of Education, Culture and Sports of Spain, for the Training of University Teachers (ref. FPU14/01523). This study forms part of the activities of the Geochemical Modelling Group (University of Zaragoza; Aragón Government). The comments and suggestions of Dr. N. Spycher and of two anonymous reviewers have contributed to improve the work and are gratefully appreciated.

8. REFERENCES

Alçiçek, H., Bülbül, A., & Alçiçek, M. C. (2016). Hydrogeochemistry of the thermal waters from the Yenice Geot Field (Denizli Basin, Southwestern Anatolia, Turkey). J. Volcanol. Geotherm. Res., 309, 118–138.

661 Alçiçek, H., Bülbül, A., Brogi, A., Liotta, D., Ruggieri, G., Capezzuoli, E., Meccheri M, Yavuzer, I.,
662 Alçiçek, M. C. (2017). Origin, evolution and geothermometry of the thermal waters in the Gölemezli
663 Geothermal Field, Denizli Basin (SW Anatolia, Turkey). J. Volcanol. Geotherm. Res., 349, 1–30.

664 Alonso, A., Floquet, M., Mas, R. and Melendez, A. (1993). Late Cretaceous carbonate platforms:
665 origin and evolution, Iberian Range, Spain. In: Masse, J.P. (Ed.), AAPG Spec. Publ., 56, pp. 297–316.

666 Apollaro, C., Dotsika, E., Marini, L., Barca, D., Bloise, A., de Rosa, R., Doveri, M., Lelli, M., Muto,
667 F. and (2012). Chemical and isotopic characterization of the thermomineral water of Terme Sibarite
668 springs (Northern Calabria, Italy). Geochem. J. 46, 117–129.

669 Appelo, C.A.J. and Postma, D. (2005). Geochemistry, Groundwater and Pollution, 2nd ed. ed. A.A.
670 Balkema, Rotterdam.

671 Arnorsson, S., Gunnlaugsson, E. and Svavarsson, H. (1983). The chemistry of geothermal waters in
672 lceland. IlI. Chemical geothermometry in geothermal investigations. Geochim. Cosmochim. Acta, 47,
673 567-577.

674 Auqué, L.F., Acero, P., Gimeno, M.J., Gómez, J, and Asta, M.P. (2009). Hydrogeochemical modeling
675 of a thermal system and lessons learned for CO2 geologic storage. Chem. Geol., 268, 324-336.

676 Aurell, M., Melendez, G., Oloriz, F., Badenas, B., Caracuel, J.E., Garcia-Ramos, J.C., Goy, A.,
677 Linares, A., Quesada, S., Robles, S., Rodríguez-Tovar, F.J., Rosales, I., Sandoval, J., Suarez de Centi,
678 C., Tavera, J.M. and Valenzuela, M. (2002). Jurassic. In: Gibbons, W. and Moreno, T. (Eds.), The
679 Geology of Spain. Geological Society of London, London, UK

680 Blasco, M., Auqué, L.F. and Gimeno, M.J. (2016). Caracterización geoquímica del proceso de mezcla
681 de aguas termales y no termales en los manantiales de Jaraba (Aragón, España). Geotemas, 16, 531-
682 534.

683 Blasco, M., Auqué, L.F., Gimeno, M.J., Acero, P. and Asta, M.P. (2017). Geochemistry,
684 geothermometry and influence of the concentration of mobile elements in the chemical characters of

carbonate-evaporitic thermal systems. The case of the Tiermas geothermal system (Spain). Chem. Geol. 466, 696-709.

Blasco, M., Gimeno, M.J., Auqué, L.F. (2018). Low temperature geothermal systems in carbonate-evaporitic rocks: mineral equilibria assumptions and geothermometrical calculations. Insights from the Arnedillo thermal waters (Spain). Sci. Total Environ, 615, 526-539.

Busby, J.F., Plummer, L.N., Lee, R.W. and Hanshaw, B.B. (1991). Geochemical evolution of water in the Madison Aquifer in parts of Montana, South Dakota, and Wyoming. U.S. Geological Survey Professional Paper 1273-F., 89 pp.

Carpenter, A.B. (1980). The chemistry of dolomite formation I: the stability of dolomite, in: Zenger, D.H., Dunham, J.B., Ethington, R.L. (Eds.), Concepts and Models of Dolomitization. Society of Economic Paleontologists and Mineralogists Spec. Publ. 28, pp. 111–121.

Chiodini, G., Frondini, F. and Marini, L. (1995). Theoretical geothermometers and PCO2 indicators for aqueous solutions coming from hydrothermal systems of medium-low temperature hosted in carbonate-evaporite rocks. Application to the thermal springs of the Etruscan Swell. Italy. Appl. Geochem., 10, 337–346.

Clark, I. and Fritz, P. (1997). Environmental Isotopes in Hydrogeology. CRC Press/Lewis Publishers, Boca -Raton (Florida).

D´Amore, F., Fancelli, R. and Caboi, R. (1987). Observations of the application of chemical geothermometers to some hydrothermal systems in Sardinia. Geothermics, 16, 271-282.

De Toledo, F.O. and Arqued, V. (1990). Estudio de los recursos hidraúlicos subterráneos de los acuíferos relacionados con la provincia de Zaragoza. Unidad Hidrogeológica 43, Sierra del Solorio. MOPU, 09.803.183/0411. 224 pp.

Fernández, J., Auqué, L. F., Sánchez Cela, V. S., & Guaras, B. (1988). Las aguas termales de Fitero (Navarra) y Arnedillo (Rioja). Análisis comparativo de la aplicación de técnicas geotermométricas

709 químicas a aguas relacionadas con reservorios carbonatado-evaporíticos. Estudios Geológicos, 44,
710 453–469.

711 Fernández, M., Marzán, I., Correia, A. and Ramalho, E. (1998). Heat flow, heat production, and
712 lithospheric thermal regime in the Iberian Peninsula. Tectonophysics, 291, 29-53.

713 Fouillac, C. and Michard, G. (1981). Sodium/Lithium ratio in water applied to geothermometry of
714 geothermal reservoirs. Geothermics, 10, 55-70.

715 Fournier, R.O. (1977). Chemical geothermometers and mixing models for geothermal systems.
716 Geothermics 5, 41–50.

717 Fournier, R.O. (1979). A revised equation for the Na-K geothermometer. Geotherm. Resour. Counc.
718 Trans. 3, 221–224.

719 Fournier, R.O. (1981). Application of water geochemistry to geothermal exploration and reservoir
720 engineering. In: Rybach, L. and Muffler, L.J.P. (Eds.), Geothermal systems: Principles and case
721 histories. John Willey & Sons Ltd., pp. 109-141.

722 Fournier, R.O. (1982). Water geothermometers applied to geothermal energy. In: D'Amore, F. (Co-
723 ordinator), Applications of Geochemistry in Geothermal reservoir Development. UNITAR/UNDO
724 centre on Small Energy Resources, Rome, Italy. pp. 37-69.

725 Fournier, R.O. and Potter II, R.W. (1982). A revised and expanded silica (quartz) geothermometer.
726 Geotherm. Res. Coun. Bull., 11, 3–12.

727 Fournier, R.O., and Potter II, R. W (1979). Magnesium correction to Na-K-Ca geothermometer.
728 Geochim. Cosmochim. Acta, 43, 1543-1550.

729 Fournier, R.O. and Truesdell, A.H. (1973). An empirical Na–K–Ca geothermometer for natural
730 waters. Geochim. Cosmochim. Acta 37, 1255–1275.

731 Giggenbach, W.F. (1988). Geothermal solute equilibria. Derivation of Na-K-Mg-Ca
732 geoindicators. Geochim. Cosmochim. Acta, 52, 2749–2765.

733 Giggenbach, W.F., Gonfiantini, R., Jangi B.L. and Truesdell, A.H. (1983). Isotopic and chemical
734 composition of Parbati Valley geothermal discharges, NW-Himalaya, India. Geothermics, 12, 199-
735 222.

736 Gökgöz, A. and Tarcan, G. (2006). Mineral equilibria and geothermometry of the Dalaman–Köycegiz
737 thermal springs, southern Turkey. Appl. Geochemistry 21, 253–268.

738 Goldscheider N, Mádl-Szőnyi J, Erőss A, Schill E (2010) Review: thermal water resources in
739 carbonate rock aquifers. Hydrogeol. J., 18, 1303–1318.

740 Helgeson, H.C., Delany, J.M., Nesbitt, H.W. and Bird, D.K. (1978). Summary and critique of the
741 thermodynamic properties of rock-forming minerals. Am. J. Sci., 278, 229 pp.

742 Henley, R.W., Truesdell, A.H., Barton, P.B. and Whitney, T. (1984). Fluid mineral equilibria in
743 hydrothermal systems. Reviews in Economic Geology I. Published by the Soc. of Economic
744 Geologists.

745 Hyeong, K. and Capuano, R.M. (2001). Ca/Mg of brines in Miocene/Oligocene clastic sediments of
746 the Texas Gulf Coast: buffering by calcite/disordered dolomite equilibria. Geochimica et
747 Cosmochimica Acta, 65, 3065–3080.

748 IGME (1980). Informe hidrogeológico del subsistema acuífero Sierra del Solorio (Sistema acuífero
749 57).

750 IGME (1982). Estudio de las manifestaciones termales de Extremadura, Salamanca, Aragón y Rioja,
751 orientados a su posible explotación como recursos geotérmicos. Informe Interno número 747.
752 Ministerio de Industria y Energía, Madrid.

753 IGME (1987). Estudio de detalle del borde septentrional de la Sierra del Solorio (Sistema acuífero 57).

754 IGME (1991). Daroca. Mapa Geológico de España. Escala 1: 200.000. Instituto Tecnológico
755 Geominero de España, 239 pp.

756 IGME (1994). Estudio de las aguas minero-medicinales, minero-industriales, termales y de bebida
757 envasada en la Comunidad Autónoma de Aragón. IGME, Madrid, 1500 p.

758 IGME (2010). Selección y caracterización de áreas y estructuras geológicas favorables para el
759 almacenamiento geológico de CO2 en España. From: http://info.igme.es/algeco2/

760 Karimi, H. and Moore, F. (2008). The source and heating mechanism for the Ahram, Mirahmad and
761 Garu thermal springs, Zagros Mountains, Iran. Geothermics 37, 84–100.

762 Kharaka Y.K. and Mariner R.H. (1988). Chemical geothermometers and their application to formation
763 waters from sedimentary basins. In: Naeser, N.D. and McCollon, T.H. (Eds.), Thermal history of
764 sedimentary basins; methods and case histories. Springer, Berlin Heidelberg New York, pp 99-117.

765 Levet, S., Toutain, J.P., Munoz, M., Berger, G., Negrel, P., Jendrzejewski, N., Agrinier, P. and
766 Sortino, F. (2002). Geochemistry of the Bagnéres-de-Bigorre thermal waters from the North Pyrenean
767 Zone sedimentary environment (France). Geofluids 2, 1–16.

768 López-Chicano, M., Cerón, J.C., Vallejos, A. and Pulido-Bosch, A. (2001). Geochemistry of thermal
769 springs, Alhama de Granada (southern Spain). Appl. Geochemistry 16, 1153–1163.

770 López, F., Cabrera, M. Cuadrat, J.M. (2007). Atlas Climático de Aragón. Gobierno de Aragón. 291 p.

771 Mariner, R.H., Evans, W.C., Young, H.W., 2006. Comparison of circulation times of thermal waters
772 discharging from the Idaho batholith based on geothermometer temperatures, helium concentrations,
773 and ^{14}C measurements. Geothermics, 35, 3–25.

774 Marini L., Chiodini G. and Cioni R. (1986). New geothermometers for carbonate-evaporite
775 geothermal reservoirs. Geothermics, 15, 71-86.

776 Meléndez, A., Meléndez, F., Portero, J. and Ramírez del Pozo, J. (1985). Stratigraphy, sedimentology
777 and paleogeography of Upper Cretaceous evaporitic-carbonate platform in the central part of the
778 Sierra Iberica. In: Milá, M.D. and Rosell, J. (Eds.), Sixtht European regional Meetring. Excursion
779 Guidebook. pp. 189-211.

780 Merino, E. and Ranson, B. (1982). Free energies of formation of illite solid solutions and their
781 compositional dependence. Clays Clay Min., 30, 29-39.

782 Michard, G. (1979). Gothermométres chimiques. Bur. Rech. Géologiques Minières (2nd Ser.), Sect.
783 III 2, 183–189.

784 Michard, G. (1983). Recueil de données thermodynamiques concernant les équilibres eaux-minéraux
785 Dans les réservoirs géothermaux. Rapp. Comm. Eur., Brussels, EUR 8590 FR.

786 Michard, G. and Bastide, J.P. (1988). Géochimie de la nappe du Dogger du Bassin de Paris. J.
787 Volcanol. Geother. Res., 35, 151.163.

788 Michard, G. and Fouillac, C. (1980). Contrôle de la composition chimique des eaux thermales
789 sulfurées sodiques du Sud de la France. In: Tardy, Y. (Ed.), Geochimique des interactions entre les
790 eaux, les minéraux et les roches. Elements, Tarbes, pp. 147-166.

791 Michard, G. and Roekens, E. (1983). Modelling of the chemical composition of alkaline hot waters.
792 Geothermics, 12, 161 169.

793 Michard, G., (1990). Behaviour of major elements and some trace elements (Li, Rb, Cs, Sr, Fe, Mn,
794 W, F) in deep hot waters from granitic areas. Chem. Geol. 89, 117–134.

795 Michard, G., Ouzounian, G., Fouillac, C. and Sarazin, G. (1979). Contrôle des concentrations en
796 aluminium disous dans les eaux des sources thermales. Geochim. Cosmochim. Acta, 43, 147-156.

797 Michard. G.. Sanjuan, B., Criaud, A., Fouillac, C.. Pentcheva, E.N.. Petrov. P.S. and Alexieva, R.
798 (1986). Equilibria and geothermometry in hot waters from granites of S. W. Bulgaria. Geochem. J.,
799 20, 159 171.

800 Minissale, A.A. and Duchi, V. (1988). Geothermometry on fluids circulating in a carbonate reservoir
801 in north-central Italy. J. Volcanol. Geotherm. Res., 35, 237-252.

802 Mohammadi, Z., Bagheri, R. and Jahanshahi, R. (2010). Hydrogeochemistry and geothermometry of
803 Changal thermal springs, Zagros region, Iran. Geothermics 39, 242–249.

804 Mutlu, H. and Güleç, N. (1998). Hydrogeochemical outline of thermal waters and geothermometry
805 applications in Anatolia (Turkey). J. Volcanol. Geotherm. Res., 85, 495–515.

806 Nemeth, K. (1963). Photometric determination of sulphate in soil extracts. Z. PflErnahr. Dung. 103,
807 193–196.

808 Nicholson, K. (2012). Geothermal Fluids: Chemistry and Exploration Techniques. Springer, Berlin
809 Heidelberg. 263p.

810 Nieva, D. and Nieva, R. (1987). Developments in geothermal energy in Mexico, part twelve. A
811 cationic composition geothermometer for prospection of geothermal resources. Heat Recov. Syst. CHP
812 7, 243-258.

813 Nordstrom, D. K., Plummer, L. N., Langmuir, L., Busenberg, E., May, H. M., Jones, B. F. and
814 Parkhurst, D. L. (1990). Revised chemical equilibrium data for major water-mineral reactions and
815 their limitation. In: Melchior, D.C. and Basset, R.L. (Eds.), *Chemical Modeling of Aqueous Systems 1/,*
816 ACS Symp. Series, 416, 398-413.

817 Palandri, J. L and Reed, M.,H. (2001). Reconstruction of in situ composition of sedimentary formation
818 waters. Geochim. Cosmochim. Acta, 65, 1741-1767.

819 Pang, Z. and Reed, M.H. (1998). Theoretical chemical thermometry on geothermal waters: problems
820 and methods. Geochim. Cosmochim. Acta, 62, 1083-1091.

821 Parkhurst, D.L. and Appelo, C.A.J. (2013). Description of Input and Examples for PHREEQC Version
822 3. A Computer Program for Speciation, Batch Reaction, One Dimensional Transport, and Inverse

Geochemical Calculations, in: U.S. Geological Survey (Ed.), Techniques and Methods, Book 6, Chap. A43. U.S. Geological Survey, Denver, Colorado.

Pastorelli, S., Marini, L. and Hunziker, J.C. (1999). Water chemistry and isotope composition of the Acquarossa thermal system, Ticino, Switzerland. Geothermics, 28, 75-93.

Peiffer, L., Wanner, C., Spycher, N., Sonnenthal, E.L., Kennedy, B.M., Iovenitti, J. (2014). Optimized multicomponent vs. classical geothermometry: Insights from modeling studies at the Dixie Valley geothermal area. Geothermics 51, 154–169.

Pinuaga, J.I., Garrido, E. and Ramírez, A. (2004). Geología, Hidrogeología y protección de los Balnearios de Jaraba (Zaragoza). Anales de la Real Academia Nacional de Farmacia, 70, 597-610.

Reed, M.H. and Spycher, N.F. (1984). Calculation of pH and mineral equilibria in hydrothermal water. Geochim. Cosmochim. Acta, 48, 1479-1490.

Reeder, R.J. (1990). Crystal Chemistry of rhombohedral carbonates. In: Reeder, R.J. (Ed.), Carbonates: Mineralogy and Chemistry. Reviews in Mineralogy, vol. 11. Mineralogical Society of America, pp. 1–47.

Reeder, R.J. (2000). Constraints on cation order in calcium-rich sedimentary dolomite. Aquat. Geochemistry 6, 213–226.Sánchez, J.A., Coloma, P. and Perez-Garcia, A. (2004). Evaluation of geothermal flow at the springs in Aragon (Spain), and its relation to geologic structure. Hydrol. J., 12, 601–609.

Sánchez, J.A., Coloma, P., Pérez-García, A. and De Leiva, A. (2000). Evaluación del flujo geotérmico en manantiales de Aragón. Geogaceta 27, 155–158.

Sanjuan, B., Michard, A. and Michard, G. (1988). Influence of the temperature of CO_2-rich springs on their Al and REE contents. Chem. Geol., 68, 57-68.

Sanz, E. and Yelamos, J.G. (1998). Methodology for the study of unexploited aquifers with thermal waters: application to the aquifer of the Alhama de Aragon Hot Spring. Ground Water, 6, 913–923.

847 Sonney, R. and Vuataz, F.D. (2010). Validation of chemical and isotopic geothermometers from low
848 temperature deep fluids of Northern Switzerland, in: Proceedings World Geothermal Congress 2010.
849 Bali, Indonesia, Indonesia, pp. 25–29.

850 Spycher, N., Peiffer, L., Sonnenthal, E.L., Saldi, G., Reed, M.H., Kennedy, B.M. (2014). Integrated
851 multicomponent solute geothermometry. Geothermics 51, 113–123.

852 Stefánsson A. and Arnórsson, S. (2000). Saturation state of feldspars in natural waters. Geochim.
853 Cosmochim. Acta, 64, 2567-2584.

854 Tena, J.M., Auqué, L.F., Gimeno, M.J. and Mandado, J. (1995). Evolución fisicoquímica y
855 geotermometría del sistema hidrotermal de Alhama-Jarba. Institución Fernando el Católico, 178 p.

856 Tole, M.P., Armannsson, H., Pang, Z. and Arnorsson, S. (1993). Fluid/mineral equilibrium
857 calculations for geothermal fluids and chemical geothermometry. Geothermics, 22, 17-37.

858 Vespasiano, G., Apollaro, C., Muto, F., Dotsika, E., de Rosa, R. and Marini, L. (2014). Chemical and
859 isotopic characteristics of the warm and cold waters of the Luigiane Spa near Guardia Piemontese
860 (Calabria, Italy) in a complex faulted geological framework. Appl. Geochemistry 41, 73–88.

861 Wang, J., Jin, M., Jia, B. and Kang, F. (2015). Hydrochemical characteristics and geothermometry
862 applications of thermal groundwater in northern Jinan, Shandong, China. Geothermics 57, 185–195.